Journal of Applied Polymer Science

Interjet Distance in Needleless Melt Differential Electrospinning with Umbellate Nozzles

Haoyi Li,[1,2] Hongbo Chen,[1] Xiangfeng Zhong,[1] Weifeng Wu,[1] Yumei Ding,[1] Weimin Yang[1,2]
[1]College of Mechanical and Electrical Engineering, Beijing University of Chemical Technology, Beijing 100029, China
[2]State Key Laboratory of Organic-Inorganic Composite, Beijing University of Chemical Technology, Beijing 100029, China
Correspondence to: W. Yang (E-mail: yangwm@mail.buct.edu.cn)

ABSTRACT: Melt electrospinning technique has shown great advantages in numerous areas where polymer dissolving, solvent accumulation, or toxicity is a concern in solution electrospinning. However, conventional capillary spinnerets in electrospinning are less productive. In this article, two needleless umbellate nozzles were used based on melt differential method, and the smallest interjet distance of 1.1 mm was observed. Experimental results indicated that the main factors affecting the interjet distance were the electric field strength and melts viscosity. The produced fiber diameter was related to interjet distance directly. Finite element modeling (FEM) showed that umbellate structure determines the intensity of maximum electric field around the rim of nozzles and the resultant interjet distance. This new method enabled the mass production of ultra-fine fibers using needleless melt electrospinning method when relatively low voltage (less than 65 kV) was loaded on the receive plate. © 2014 Wiley Periodicals, Inc. J. Appl. Polym. Sci. **2014**, *131*, 40515.

KEYWORDS: needleless electrospinning; melt eletrospinning; interjet distance; theory and modeling

Received 17 November 2013; accepted 27 January 2014
DOI: 10.1002/app.40515

INTRODUCTION

Melt electrospinning technique is under research compared with solution electrospinning technique, but shows great advantages in numerous areas, in which polymer dissolving, solvent accumulation, or toxicity is a concern.[1,2] In this context, melt electrospinning is gradually attracting more attention and becoming an alternative approach overcoming those abovementioned challenges. However, it also brings new issues to the forefront, such as high viscosity of polymer melt, relatively complicated setups, and low efficiency.[3]

The output of melt electrospinning is 10 times that of solution electrospinning,[4] but is still limited compared with melt blowing method.[5] Therefore, increasing the output of melt electrospinning becomes a concern before it gets industrialized. As shown in Figure 1, interjet distance is defined as the distance between adjacent Taylor-cone tips in needleless electrospinning process,[6] which directly decides the yield per unit spinning area. Therefore, decreasing the interjet distance is extremely meaningful to realize the mass production of ultra-fine fiber.[7] Ogata et al.[8] prepared linear arrayed fibers by the use of a melt electrospinning device, in which linear laser light was a heating source and the minimum interjet distance of 4.55 mm was measured. Komarek et al.[9] from Czech Republic University proposed "rod" and "cleft" melt electrospinning setup, where multiple jets were received onto the receiver electrode and 5.2 mm interjet distance was obtained. Inspired by "nano-spider" in Czech Republic,[10] Fang et al.[11] tried a disk partially immersed in polymer melt and produced fibers with diameter of 400 nm, but information about interjet distance was not mentioned.

Previous research indicates that interjet distance directly determines the output of fibers per unit spinning area, and that the shape of needleless nozzle has great influence on the resultant interjet distance.[12] Therefore, the key to increase the output of melt electrospinning is the design of needleless nozzle and evaluation of the resultant interjet distance. In solution electrospinning, self-organized jets from free surface has been a generalized approach. Lukas et al.[13] developed a one dimensional electrohydrodynamic theory to predict the critical electric field strength and corresponding interjet distance, and were well coincident with the experimental results. However, this method was not suitable for polymer melt because of the super high critical electric field and the theory was also not confirmed when the fluid was non-conducting polymer melt. Wang et al.[14] designed a solution needleless electrospinning device with a conical wire coil, by which the breakdown voltage was significantly lowered compared with that of free surface needleless electrospinning method, but this method was hard to expanded to melt electrospinning.

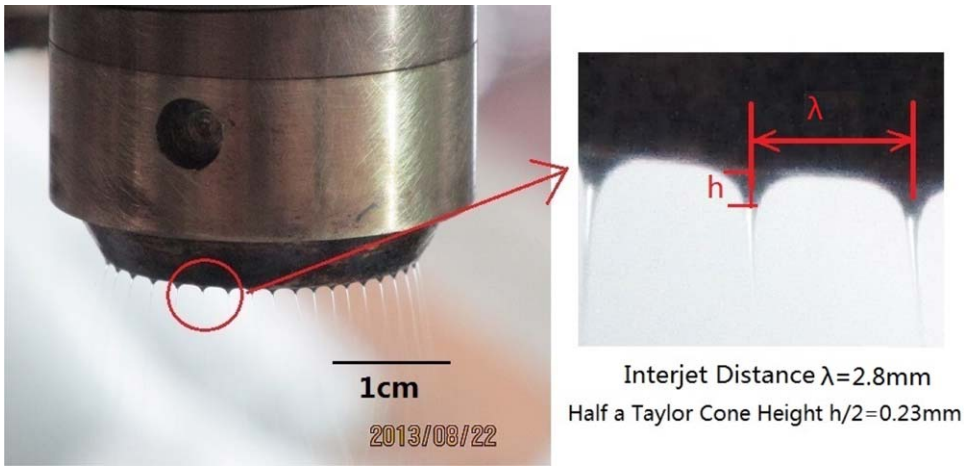

Figure 1. Definition of interjet distance λ. [Color figure can be viewed in the online issue, which is available at wileyonlinelibrary.com.]

In this work, two kinds of nozzles were used based on melt differential method, and interjet distance was experimentally studied and compared. Furthermore, theoretical analysis was performed to verify whether the interjet distance formula of needless solution electrospinning from free surface deduced by Lukas et al.[13] was suitable for the evaluation of interjet distance in needleless melt electrospinning. The design of the nozzles enabled the uniform melts distribution around circumferential fringe of umbellate nozzles, which allowed tens of uniform jets ejected from the fringe using needleless melt electrospinning method. What is more, the existence of circumferential fringe of umbellate nozzles as sharp edge contributed to charge accumulation, which permitted lower loaded voltage than conventional needleless electrospinning device. It may be a new method for nozzle designing and give rise to interest in scale-up research of melt electrospinning for ultrafine fiber production.

EXPERIMENTAL

Materials

Polypropylene (PP) with a melt flow index (MFI) of 2000 g/10 min was procured from Expert Company (China) and was used as received.

Melt Differential Electrospinning Equipment

The equipment used for melt electrospinning is shown as the section view in Figure 2(a,b). It consisted of five major components: melt inlet, melt distributor, umbellate nozzle, high voltage power supply, and receiver plate. Melt was metered and supplied into melt inlet by a self-designed micro extruder, and the melt flow rate could be controlled in the range of 1–100 g/h. Melt distributor was designed to induce the single melt flow to the circumference of the umbellate nozzle uniformly. The nozzle was earthed and high positive voltage was loaded on the receiver plate using a high voltage power supply source (Tianjin Dongwen Company) at a value range of 0–80 kV. Receiver plate was a circular copper plate with diameter of 150 mm and thickness of 3 mm.

The process was described as follows: first, the melt was transformed from a cylindrical flow into a uniform ring-like flow, next, the ring-like flow was distributed to the umbellate nozzle, then a thin and uniform melt film formed on the umbellate circumferential surface, finally, when the applied high voltage surpassed a critical value, self-organized multiple jets around the rim of the umbellate nozzle were ejected to the receiver plate spontaneously as shown in Figure 2(c,d). We termed this

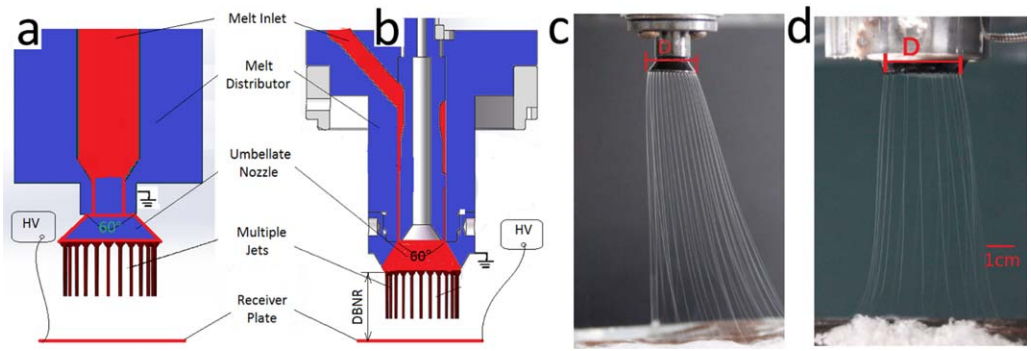

Figure 2. Schematics and pictures of melt differential electrospinning applied two kinds of nozzles: nozzle with melt distributed on the outer surface of the umbrella-like nozzle (OCS, (a, c)) and nozzle with melt distributed on the internal surface of the umbrella-like nozzle (ICS, (b, d)). [Color figure can be viewed in the online issue, which is available at wileyonlinelibrary.com.]

process as melt differential electrospinning because of a melt flow was self-organized and divided into tens of minor Taylor-cones under the stretching force of electric field.

Two kinds of nozzles were used and tested to generate multiple jets. One was a nozzle with melt distributed on the internal surface of the umbrella-like nozzle as shown in Figure 2(d) and was called ICS nozzle for short. Another was a nozzle with melt distributed on the outer surface of the umbrella-like nozzle as shown in Figure 2(c) and was called OCS nozzle for short. The bottom rim diameters of the two umbellate nozzles were 26 and 16 mm, respectively, and both of them had same cone angle (60°).

Other affiliated components included electrical heating system and controlling system. The extruder, melt distributor, and nozzle were earthed, which allowed them to be designed into complicated system and heated by electrical heating elements directly.[4] The two umbellate nozzle structures mentioned above were used to compare the effect of electrical field and melt viscosity on interjet distance. The effect of applied voltage on receiver plate was tested when nozzle temperature was set to a constant value of 250°C, distance between nozzle and receiver plate (spinning distance) was set to a constant value of 13 cm, and applied voltage on receiver plate was set around 25–65 kV. The effect of spinning distance on the interjet distance was observed when nozzle temperature was set to a constant value of 250°C, applied voltage on receiver plate was set to a constant value of 40 kV, and spinning distance was set around 50–13 cm with 15 mm interval. The effect of polymer melt viscosity on interjet distance was indirectly manipulated by changing nozzle temperate at the range of 180–260°C when spinning distance was set to 100 mm and applied voltage on receiver plate was set to 40 kV. Relationship between fiber diameter and interjet distance was showed by measuring the fiber diameters when the spinning distance was set to 11 cm, ICS nozzle temperature was set at 260°C, and applied voltage was set between 39 and 63 kV.

Fluid flow rate was an important factor influencing the final fiber diameter either in solution or in melt electrospinning with single jet. However, fluid flow rate have no effect on interjet distance in needleless solution electrospinning.[13] Our basic experiment confirmed this result in needleless melt electrospinning, in which, the interjet distance remained the same as the PP melt flow rate changed from 4.5 to 36 g/h for both kinds of umbellate nozzles at different conditions. For simplicity, all the experiments in this article were performed at a fixed inlet PP melt flow rate of 12.5 g/h for each nozzle.

Characterization

As Figure 3 shows, three pictures of multiple jets under each melt differential electrospinning process condition were captured or photographed by camera (Cannon 600D) at 6X magnification, and then the jets around the nozzles were numbered and averaged, at last the interjet distance (λ) was calculated using the value of bottom rim diameters of the umbellate nozzles (D) and averaged jets number (N) by equation: $\lambda = \pi D/N$.

In this article, polymer melts at the surface of umbellate nozzles were free of any shear force, therefore, the viscosity of PP6820 was tested with an DHR-2 Rheometer (TA Instrumental Company) at a low shear rate of 0.1 rad/s. Measurements were performed in a temperature scanning mode ranging from 190 to 280°C under nitrogen protection. Distance between plates was set to 1 mm.

Diameters of electrospun PP fibers were examined by scanning electron microscopy (SEM) (S-4700, Hitachi, Japan). Before observation, all fibers were platinum coated. Image processing software (Image J 2X) was applied to calculate the average fiber diameters and standard deviations from 40 measurements of each sample.

RESULTS AND DISCUSSION

Effect of Uniform Electric Field Strength on Interjet Distance in Melt Differential Electrospinning

In melt differential electrospinning, the viscosity of polymer melt is much higher than that of solution electrospinning, so higher electrical electric field strength is applied in melt differential electrospinning than that in solution electrospinning. In solution electrospinning of free surface, applied voltage was three to five times higher than that of solution electrospinning of single needle. Therefore, to avoid breakdown, optimizing nozzle structure and lowering the applied voltage of needleless melt electrospinning were worth trying.

In a conventional attempt, the evaluation of impact of electric field strength was always performed by easily assuming that the electric field strength was a uniform electric field (ratio of loaded voltage to spinning distance)[15,16] In this work, either the increase of applied voltage or the decrease of spinning distance both could result in an increase of uniform electrical field intensity, which could conquer high surface tension of polymer melt and attain more fibers. As Figure 3(a) shows, interjet distances in melt differential electrospinning using ICS or OCS nozzle were decreased with the increase of applied voltage when the spinning distance was fixed at 13 cm. However, interjet distance in melt differential electrospinning using OCS nozzle was extremely shorter than that of ICS nozzle. The former was only 1.2 mm [Figure 3(c)] when 55 kV voltage was applied, while the latter was 3 mm [Figure 3(b)] when 65 kV voltage was applied. As Figure 3(d) shows, interjet distances in melt differential electrospinning using ICS or OCS nozzle were decreased with the decrease of spinning distance when applied voltage was fixed at 40 kV. The latter was only 1.2 mm [Figure 3(f)] when spinning distance was set to 5 cm, while the former was 2.8 mm [Figure 3(e)] when spinning distance was set to 7 cm, and the interjet distance variation of the former was more sensitive than that of the latter, which means that the electrical field variation of ICS nozzle was greater than that of OCS nozzle. Not only uniform electric field strength could affect the interjet distance, but the spinning distance variation with fixed uniform electric field strength (5 kV/cm) could also affect the interjet distance to some extent. Figure 3(g) shows that interjet distance decreased with the increase of spinning distance until 7 cm, and then the interjet distance became constant when the spinning distance was between 7 and 13 cm [Figure 3(h,i)]. In electrospinning, the generation of Taylor-cones and multiple jets was the result of electrical force, surface tension, and gravity. Both

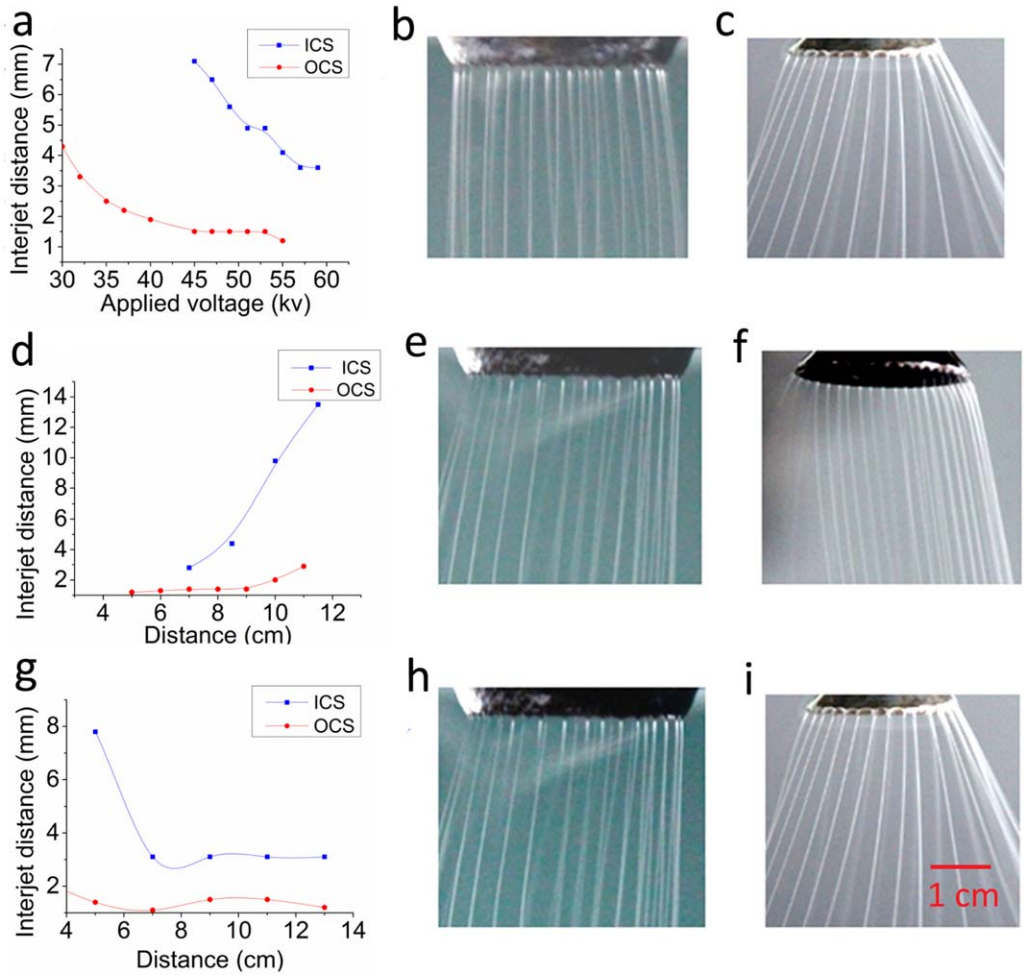

Figure 3. Comparison of interjet distances and corresponding photos with smallest interjet distance using ICS and OCS nozzles under different conditions: (a–c) changing applied voltage when the spinning distance was fixed at 13 cm; (d–f) changing spinning distance when applied voltage was fixed at 40 kV; (g–i) changing spinning distance and applied voltage when the uniform electric field strength was fixed at 5 kV/cm (all the deviations of above calculated interjet distances were minor than 0.15 mm). [Color figure can be viewed in the online issue, which is available at wileyonlinelibrary.com.]

of the increase of loaded voltage and the decrease of spinning distance caused the strengthen of electrical force, which could explain why the interjet distance decreased for both nozzles. To explain why the ICS nozzle had larger interjet distance, considering the accumulation of charge at the sharp edge of nozzles, the maximum electric field strength was necessary to evaluate.

Effect of Maximum Electric Field Strength on Interjet Distance in Melt Differential Electrospinning

The above experiments and phenomenon demonstrated that electric field strength played an important role in determining the final interjet distance, even if a constant uniform electric field strength was applied, the final interjet distance changed with the increase of spinning distance, by which it was assumed that the maximum electric field strength and distribution at the bottom rim regions of both nozzles greatly affected the final interjet distance. To further prove this judgment, finite element analysis using electric module in ANSYS12.1 was performed. The electric field strength profiles of two needleless umbellate nozzles at different spinning distances with constant uniform electric field strength of 5 kV/cm were simulated.

The models of two types of nozzles were simplified as shown in Figure 4 and the basic analysis parameters used were listed in Table I. As shown in Figures 5(a) and 7(b), the electric field strength at different area of the same nozzle varied. Figure 5(c,d) showed the magnified partial view of electric field strength distribution at the bottom rim of ICS and OCS nozzles. The maximum electric field strength was formed on the bottom rim of nozzles and much lower electric field strength was established close to the receiver plate. As Figure 6 shows, for both kinds of nozzles, the maximum electric field strength increased with the increase of spinning distance, which actually explained why the interjet distance decreased when the spinning distance altered with fixed uniform electric field strength of 5 kV/cm. However, the maximum electric field strength for OCS nozzle was much higher than that for ICS nozzle, which was the same under previous conditions. It was interesting to find that all the rims of nozzles where fibers generated had high

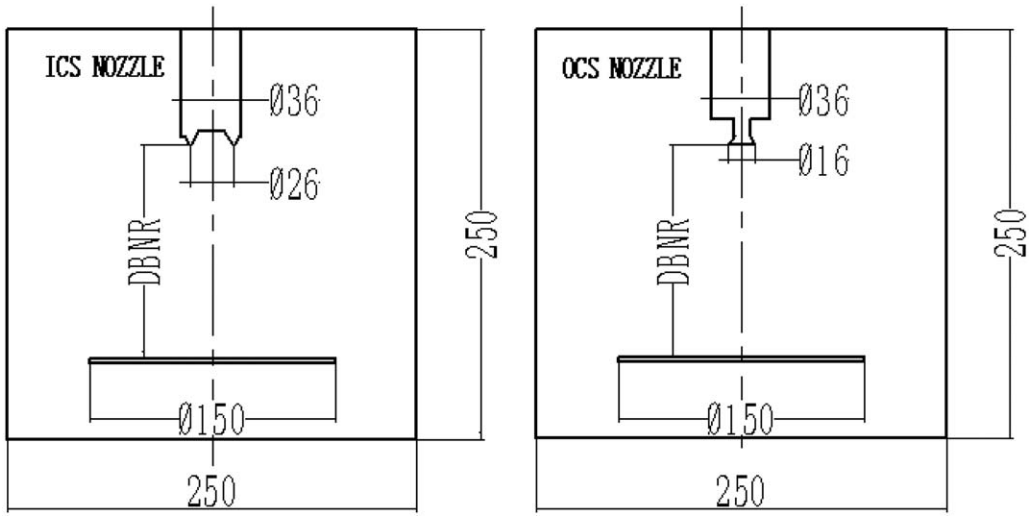

Figure 4. Modeling of two nozzles for finite element analysis (units : mm).

Table I. Parameter Setting of Finite Element Analysis

Element type	Boundary dimensions	Relative dielectric constant of air
2D Quad121	260 × 260 mm	1
Voltage on nozzle(V)	Voltage on receiver plate (kV)	DBNR (mm)
0	15, 25, 35, 45	30, 50, 70, 90

electric field strength. Even so, we still could not explain why interjet distance of OCS nozzle was much shorter than that of ICS nozzle while the same maximum electric field strength occurred on the latter one. It was assumed that this phenomenon was related to thickness of the melt layer around the nozzle. Subsequent research will be conducted to show the internal mechanism.

Effect of Melt Viscosity on Interjet Distance in Melt Differential Electrospinning

Since solution viscosity was the one of the main factors determining the interjet distance in needleless electrospinning from free surface, in this study, the effect of melt viscosity on interjet distance in melt differential electrospinning was evaluated. PP melt viscosity was obviously related to temperature, so the effect of melt viscosity on interjet distance was controlled by varying the nozzle temperature indirectly. Mutual relation between

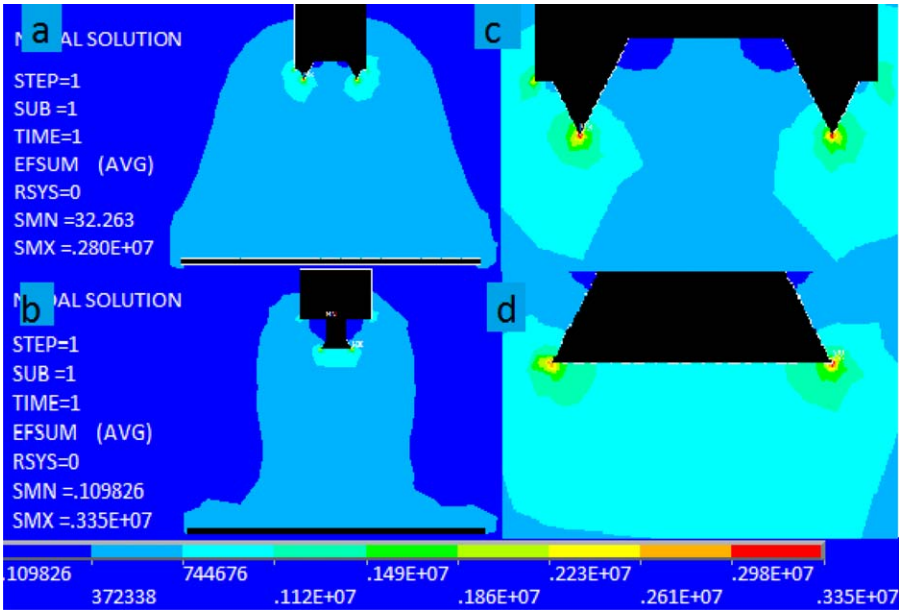

Figure 5. Diagram of electric field strength of ICS (a) and OCS (b) nozzles (Ansys simulation condition: 45 kV applied voltage and 90 mm spinning distance.) and the magnified partial view of electric field strength distribution at the bottom rim of ICS (c) and OCS (d) nozzles. [Color figure can be viewed in the online issue, which is available at wileyonlinelibrary.com.]

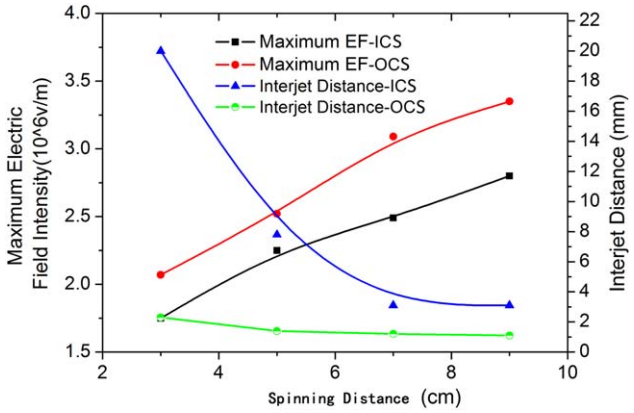

Figure 6. Maximum electric field intensity and real interjet distance of two kinds of nozzles simulated and tested when uniform field intensity was set to 0.5×10^6 v/m with varied spinning distance. [Color figure can be viewed in the online issue, which is available at wileyonlinelibrary.com.]

temperature and melt viscosity was illustrated as shown in Figure 7(a), in which temperature was started at 190°C and ended at 280°C, and viscosity continuously decreased from 9 to 2 Pa.s. Experiment was performed at various temperatures with a constant applied voltage of 40 kV and a constant spinning distance of 10 cm. As Figure 7(b) shows, interjet distance increased with the increasing temperature. For OCS nozzle, the interjet distance changed from 1.5 to 1.1 mm, then remained at 1.1 mm after temperature surpassed 250°C. For ICS nozzle, the interjet distance changed from 7 to 4.4 mm, then kept at 4.4 mm after temperature surpassed 230°C. Experimental data showed the effect of viscosity on resultant interjet distance. It was noted that the interjet distance did not change when the viscosity reached a certain value, which means that finite lowering of melt viscosity was effective to the scaling-up production. It was also noted that interjet distance of ICS nozzle was more dependent on melt viscosity than that of OCS nozzle, since the former decreased 37% in value while the latter only decreased 10%.

Relationship between Fiber Diameter and Interjet Distance

In conventional single-jet electrospinning process, the resultant fiber diameter was directly related to inlet flow rate and had little relation to other parameters.[17] In this melt differential electrospinning system, the single supplied melt flow was distributed around the circumferential surface of nozzle, and then multiple jets were ejected out from the nozzle when applied voltage was over critical value. This meant that when a fixed melt flow was supplied, the fiber diameter decreased with the decrease of interjet distance, or the increase of jets number.

Table II. Relationship between Fiber Diameter and Interjet Distance

Number	Applied voltage (kV)	Jets number	Interjet distance (mm)	Average fiber diameter (μm)	Standard deviation (mm)
1	39	14	5.8	14.6	3.3
2	43	20	4.1	14.1	3.8
3	47	28	2.9	12.5	3.6
4	51	34	2.4	12.1	1.0
5	55	48	1.7	12.0	0.9
6	59	56	1.5	8.8	0.7
7	63	60	1.4	5.3	0.6

The interjet distance was controlled by increase voltage from 37 to 63 kV with a fixed spinning distance of 11 cm as shown in Table II, and the resultant fibers were collected at every 4 kV interval. It can be found in Figure 8 that the smaller the interjet distances, the smaller the fiber diameter. The smallest interjet distance of 1.4 mm and the average fiber diameter of 5.3 μm were obtained at the highest applied voltage of 63 kV before breakdown. It can be also found in Figure 8 that the standard deviations of fiber diameter were quite larger below applied voltage of 50 kV while that above 50 kV were a little small. It can be explained that when the larger electrical force loaded on the melt flow was beneficial to the melt flow distribution, which contribute to the obtain of more uniform fiber diameter. Relationship between fiber diameter and interjet distance indicated that this melt differential method contributed to obtain smaller fibers, especially when a larger electrical force was loaded on the melt flow.

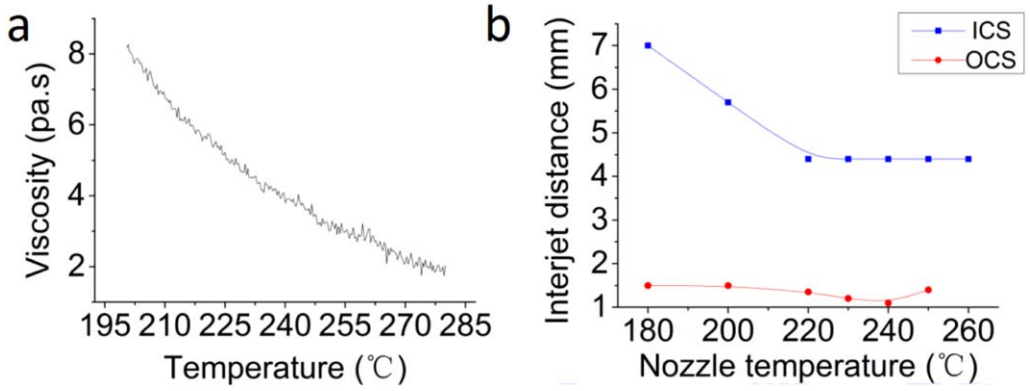

Figure 7. Diagram of polymer melts viscosity (a) and interjet distance (b) at different nozzle temperature. [Color figure can be viewed in the online issue, which is available at wileyonlinelibrary.com.]

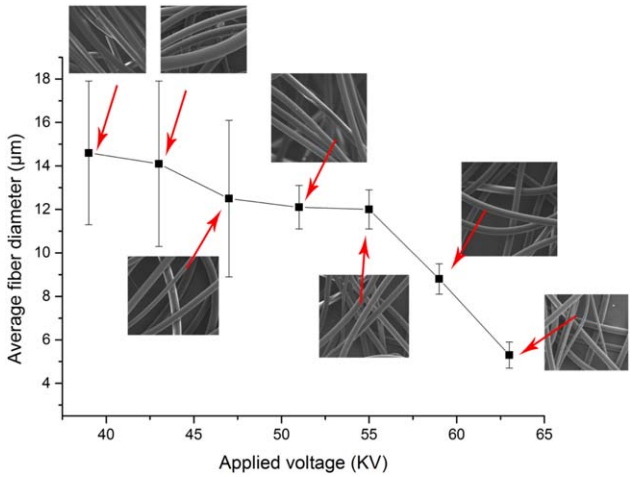

Figure 8. Fiber diameter at different applied voltages. [Color figure can be viewed in the online issue, which is available at wileyonlinelibrary.com.]

Theoretical Analysis of Interjet Distance in Needleless Melt Differential Electrospinning

Preparation of ultra-fine fiber by electrospinning from polymer solutions or melts is originated from the phenomenon known as electro-hydrodynamic atomization. Although there were differences in the elongation of the melt jet and in the mechanism of charging between melt electrospinning and solution electrospinning, the principle of the formation of the Taylor-cones is believed to be universal. The Taylor-cone is formed on the melt surface if the electrostatic pressure overcomes the surface tension forces, and the jet originates when the electric field force surpasses the certain critical force.[18]

Take ICS nozzle for example. As Figure 9 shows, by spreading the internal surface of the ICS nozzle, a sector could be formed, the long arc of the sector was right the circular bottom rim of the nozzle. It can be then assumed as a straight line with multiple jets originated along the line uniformly. Define this straight line as x axis, and the length of the line as $L=\pi D$. In this condition, the Taylor-cones on the nozzle can be seen as a one-dimensional wave perpendicular to x axis. On the basis of electro hydrodynamics, the wave's vertical displacement along the z axis is described using the periodic real part of a complex quantity ξ:

$$\xi = A\exp\left[i(kx-\omega t)\right] \tag{1}$$

In which the symbols A, k, ω, and t stand for amplitude, wave number, angular frequency, and time, respectively. It can be also described like this:

$$\xi = Ae^{qt}\exp(ikx) \tag{2}$$

When the electrical field intensity E_o exceeds the critical electrical field intensity E_c, the square of the angular frequency ω^2 becomes negative and so, ω becomes purely imaginary. The imaginary angular frequency is defined as $q=\mathrm{Im}(\omega)$.

Originally, the melts on the surface of nozzle is subjected to fields of surface tension, gravitation and electricity, and a non-zero curvature called a Taylor-cone will be formed. The Euler equation and related dispersion law, which governs the dynamic balance of the relevant forces, was derived previously[13] by making the assumptions as follows: a velocity field $\vec{v}=\vec{v}[x(t), y(t), z(t), t]$, the melt flow is a potential one, that is, $\nabla\times\vec{v}=0$, that is $\vec{v}=\nabla\phi$, and the melt is an incompressible one, that is, ρ (melt density) is constant, and the amplitude A of the wave is initially negligibly small, as compared with its wavelength λ. These aspects simplify the Euler equation into the following form:

$$\nabla\left(\rho\frac{\partial\phi}{\partial t}+p\right)=0 \tag{3}$$

where p stand for the pressure. This equation can be further simplified by decomposing the pressure into hydrostatic pressure $P_h=\rho g\xi$, capillary pressure $P_C=-\gamma\left(\partial^2\xi/\partial X^2\right)$, and electric pressure $P_e=\varepsilon E^2/2$, where$\varepsilon$is relative permittivity of the surrounding gas, E is the intensity of the electric field, and γ is the surface tension.

$$\omega^2=\left(\rho g+\gamma k^2-\varepsilon {E_0}^2 k\right)k/\rho \tag{4}$$

The critical condition can be deduced by setting $\omega^2=0$ and $\partial\omega/\partial k=0$. After rearranging, the critical value of wave number k is can be deduced as $k_c=\varepsilon {E_0}^2/2\gamma$, and E_c for unstable wave is:

$$E_C=\sqrt[4]{4\gamma\rho g/\varepsilon^2} \tag{5}$$

The minimal value of ω^2 with respect to k is obtained by solving $\partial\omega^2/\partial k=0$ and two solutions k_1 and $k_2$are expressed as

$$k_{1,2}=\left[2\varepsilon {E_0}^2\pm\sqrt{\left(2\varepsilon {E_0}^2\right)^2-12\gamma\rho g}\right]/6\gamma \tag{6}$$

The average interjet distance can be then expressed by terms of wave length $\gamma=2\pi/k$, where k is assigned the larger value.

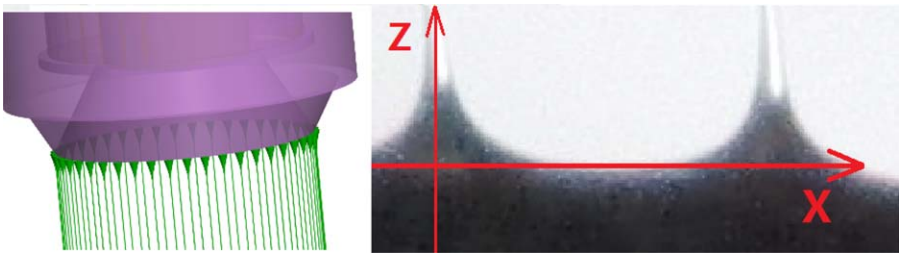

Figure 9. Sketch of the ICS nozzle and definition of x and z axis after the Taylor-cones were spread. [Color figure can be viewed in the online issue, which is available at wileyonlinelibrary.com.]

Table III. Properties of PP6820 and Comparison between Theoretical and Experimental Results

Parameters	$\lambda(Nm^{-1})$	$\rho(kg/m^3)$	$g(ms^{-2})$	$\varepsilon(Fm^{-1})$	$\lambda_c(m.10^{-3})$	$E_c(Vm^{-1})$	$E_0(Vm^{-1})$	$\lambda_0(m.10^{-3})$
Theoretical	0.025	750	10	8.85×10^{-12}	19.8	1.68×10^6	3.06×10^6	2.4
Experimental	-	-	-	-	26.4	1.88×10^6	3.06×10^6	3.0

$$\lambda_0 = 12\pi\gamma/[2\varepsilon E_0{}^2 \pm \sqrt{(2\varepsilon E_0{}^2)^2 - 12\lambda\rho g}] \quad (7)$$

On the basis of the eq. (7) of average interjet distance governed by material properties like γ, ρ, and real value of applied electrical field intensity E_0, the theoretical calculation and experimental results were compared. In this case, the value of the critical voltage and interjet was measured directly for the needless melt differential electrospinning using ICS nozzle described previously. The experimental was performed when nozzle temperate was set to 230°C, spinning distance was set to 85 mm, and applied voltage was set to 40 kV. The basic properties of PP6820 were listed in Table III E_c and E_0 used here for calculation were the simulated real maximum electrical value by ANSYS12.1 as used previously. It was found that the theoretical calculated results were close to experimental results, but the experimental critical electrical field intensity and interjet distance was a little larger than theoretical calculated value. It was assumed that this was the result of the difference of melts distribution caused by the nozzle structure. Therefore, further investigation is needed to figure out the relationship between the nozzle structures and melt distribution, and the melt film thickness around surface of umbrella nozzles.

CONCLUSION

Two kinds of nozzle structures were used on the base of needleless melt differential electrospinning method for generating multiple jets. Experimental research demonstrated that the applied voltage and viscosity both have an influence on the interjet distances. Smallest interjet distances of 1.1 and 1.4 mm were attained using OCS and ICS nozzles, respectively, which were about one quarter of that attained by using "rod" and "cleft" melt electrospinning setup.[9] Comparison of two nozzles showed that OCS nozzle had a smaller interjet distance under lower loaded voltage and this phenomenon was confirmed by FEM simulation. But there was no evidence to explain why OCS nozzle could generate more jets under the same condition. It was assumed that this phenomenon was related to the thickness of the melts film around the umbellate surface of the nozzles caused by the action of gravity. It was found that the theoretical calculated results were close to experimental results, but the experimental critical electrical field intensity and interjet distance was a little larger than theoretical calculated value. Therefore, further research and theoretical simulation should be performed to study and solve the inner mechanism of these phenomena.

REFERENCES

1. Hutmache, D. W.; Dalton, P. D. *Chem. Asian J.* **2011**, *6*, 44.
2. Teo, W. E.; Ramakrishna, S. *Nanotechnology* **2006**, *17*, 89.
3. Lyons, J.; Ko, F. *Polym. News* **2005**, *30*, 170.
4. Deng, R.; Liu, Y.; Ding, Y.; Xie, P.; Luo, L.; Yang, W. *J. Appl. Polym. Sci.* **2009**, *114*, 166.
5. Shambaugh, R. L. *Ind. Eng. Chem. Res.* **1988**, *27*, 2363.
6. Taylor, G. *Royal Soc. Proc. A* **1964**, *280*, 383.
7. Zhou, F.; Gong, R.; Porat, I. *Polym. Int.* **2009**, *58*, 331.
8. Shimada, N.; Yamaguchi, S.; Nakane, K.; Ogata, N. *J. Appl. Polym. Sci.* **2010**, *116*, 1282.
9. Komarek, M.; Martinova, L. Design and Evaluation of Melt-Electrospinning Electrodes. In Proceedings of 2nd NANOCON International Conference, Olomouc, Czech Republic, EU, **2010**; p 72.
10. Petrik, S.; Maly, M. In Proceedings of 2009 Fall MRS Symposium, MIT Press: Boston, MA, **2009**.
11. Fang, J.; Zhang, L.; Sutton, D.; Wang, X.; Lin, T. *J. Nanomater.* **2012**, 2012, 1.
12. Fuh, Y. K.; Lien, L. C. *Micro. Nano. Lett.* **2012**, *7*, 1088.
13. Lukas, D.; Sarkar, A.; Pokorny, P. *J. Appl. Phys.* **2008**, *103*, 084309.
14. Wang, X.; Niu, H.; Lin, T. *Polym. Eng. Sci.* **2009**, *49*, 1582.
15. Lyons, J.; Li, C.; Ko, F. *Polymer* **2004**, *45*, 7597.
16. Rangkupan, R.; Reneker, D. H. *J. Metals Mater. Miner.* **2003**, *12*, 81.
17. Subbiah, T.; Bhat, G. S.; Tock, R. W.; Parameswaran, S.; Ramkumar, S. S. *J. Appl. Polym. Sci.* **2005**, *96*, 557.
18. Rayleigh, L. *Edinburgh Dublin Philo. Magazine J.* **1882**, *44*, 184.